

# Data Distributional Properties As Inductive Bias for Systematic Generalization

Felipe del Río

Pontificia Universidad Católica de Chile  
fidelrio@uc.cl

Daniel Florea

Pontificia Universidad Católica de Chile  
dflorea@uc.cl

Julio Hurtado

University of Warwick  
julio.hurtado@warwick.ac.uk

Alain Raymond-Sáez

Pontificia Universidad Católica de Chile  
afraymon@uc.cl

Rodrigo Toro Icarte

Pontificia Universidad Católica de Chile  
rntoro@uc.cl

Cristián Buc Calderón

CENIA  
cristian.buc@cenia.cl

Álvaro Soto

Pontificia Universidad Católica de Chile, CENIA  
asoto@ing.puc.cl

## Abstract

Deep neural networks (DNNs) struggle at systematic generalization (SG). Several studies have evaluated the possibility to promote SG through the proposal of novel architectures, loss functions or training methodologies. Few studies, however, have focused on the role of training data properties in promoting SG. In this work, we investigate the impact of certain data distributional properties, as inductive biases for the SG ability of a multi-modal language model. To this end, we study three different properties. First, data diversity, instantiated as an increase in the possible values a latent property in the training distribution may take. Second, burstiness, where we probabilistically restrict the number of possible values of latent factors on particular inputs during training. Third, latent intervention, where a particular latent factor is altered randomly during training. We find that all three factors significantly enhance SG, with diversity contributing an 89% absolute increase in accuracy in the most affected property. Through a series of experiments, we test various hypotheses to understand why these properties promote SG. Finally, we find that Normalized Mutual Information (NMI) between latent attributes in the training distribution is strongly predictive of out-of-distribution generalization. We find that a mechanism by which lower NMI induces SG is in the geometry of representations. In particular, we find that NMI induces more parallelism in neural representations (i.e., input fea-

tures coded in parallel neural vectors) of the model, a property related to the capacity of reasoning by analogy.

## 1. Introduction

Humans excel at adapting quickly to novel tasks. This feature emerges from our *systematic generalization* (SG) ability, that is, the flexible recombination of previous (blocks of) knowledge in ways that allow us to behave effectively under novel task demands and, more generally, help us make sense of the world [21, 46].

Importantly, SG depends on prior knowledge or inductive biases upon which agents can rely on [40]. Indeed, inductive biases enable the representing of knowledge in the form of discrete independent concepts, which can be leveraged for flexible and rapid adaptation to new situations. In humans, for example, visual perception is strongly biased towards shapes which aids in recognizing previously unknown objects [23, 25]. This bias helps us reason independently about color, texture, or form, aiding in recognizing unknown objects regardless of their specific combination of properties. A child who has seen many horses, for instance, is likely to infer that a zebra moves similarly to a horse despite their differing colors.

In contrast to empirical observations in humans [12], SG does not emerge naturally in an i.i.d. setting in deep neural networks (DNNs) [33, 34, 37, 60]. Since training data

is always finite in machine learning, models need built-in assumptions to generalize to novel inputs. These assumptions, often called inductive biases [24], help guide models toward solutions in situations not seen during training, and promote model weight configurations (i.e., solutions) that encourage generalization aligned with specific objectives [7, 63]. Inductive biases can take different forms, such as constraints over loss functions [35], architectures [45], pre-training [14], learning [39], or the geometry of representations [29, 59, 61]. However, the role of specific training data distributional properties as inductive biases remains surprisingly understudied.

A notable exception to this trend is the study of data complexity. Indeed, both in terms of patterns and scale, increasing training data complexity can improve SG in language models [1, 20, 31, 38, 51, 65]. Similarly, within the realm of vision, augmenting training data with translations has been shown to improve learned invariances [9]. Nevertheless, several questions remain open. First, although incrementing training data complexity does promote SG, which property (or properties) of data distribution subtends this promotion remains obscure. Second, despite the tremendous success and broad applicability of vision-language models [6, 41–43], whether data training properties can boost SG in these models has not been explored. Third, a systematic analysis of the effect of training data properties on internal representations and how these can promote SG is also missing. In other words, we lack a functional explanation of how data properties may promote SG.

In this work, we focus on the following research questions: “Can SG be induced solely through changing properties of the training data? If so, how and why does this work?”. To answer these questions, we focus on a Multi-modal Masked Language Modeling (MMLM) setting and test for three different properties of the data: *diversity*, an increase in the cardinality of latent factors of the training distribution; *burstiness*, a limitation on the cardinality of latent factors in particular instances of the training data; and *latent intervention*, a targeted intervention on the value of a latent factor. We construct datasets that alter these properties by manipulating their generative latent factors and test how a model trained on these datasets generalizes to instances of unseen combinations of latent factors. Our experiments demonstrate that manipulating these properties the SG capability of a model.

Finally, to understand why these properties induce better SG, we perform a thorough set of experiments. We study the role of the Normalized Mutual Information (NMI) between latent attributes of a dataset and find that it correlates strongly with out-of-distribution (o.o.d) generalization. We then turn to the effect of data distributional properties on learned representations. Moreover, we analyze the representations’ geometry compared to baseline models. We find

that the more diverse a dataset the more it induces disentanglement in the representations. Also, we analyze other geometrical properties of representations. There is currently a conjecture —based on empirical observations of biological neural representations— that the more parallel representations remain under a particular change in a latent attribute, the better they are at SG. Through our experiments, we find that NMI tends to produce representations that show more parallelism, suggesting a mechanism by which lower NMI datasets can induce SG. Thus, our contributions can be summarized as follows:

- We show that increasing the number of values of a given data factor, a property of data we call *diversity*, promotes SG in an MMLM task. We achieve an absolute increase in accuracy of up to 89% in a systematic test set, solely through manipulation of the training data.
- Analogously, we show that probabilistically restricting the number of values of latent factors in a given input, a term we call *burstiness*, also increases SG, with an absolute 15% increase over the baseline. This increase, however, comes at the cost of decreased performance related to the restricted factor.
- We also show that intervening some of the latent factors in the training data, without violating systematicity, significantly increases SG, up to an absolute increase of 15%.
- We find that datasets with lower NMI between latent factors tend to produce models with better out-of-distribution performance. Moreover, we find that one mechanism by which they induce this behavior is by promoting the emergence of *representations with more parallelism under changes in latent attributes*.

## 2. Problem Formulation

We train a model on a similar task to CLEVR[32] to correctly respond to a textural query given contextual information (in our case, images) about a group of entities contained in it. In particular, queries that will give a partial description of the image (e.g., “small red rubber sphere, large [?] metallic cylinder, etc.”) will always resolve to predict the value of one or more particular attributes (e.g., color in this case) of a particular entity (e.g., cube). See Figure 1 for an example input image, query, and expected answer. A model able to perform SG will achieve this over a test set with unseen combinations of these attributes during training. This is relevant because models tend to memorize combinations of attributes (which may prove spurious) during training rather than learn each one separately.

### 2.1. Task formalization

Let  $A$  be a set of latent attributes  $\{a_1, a_2, \dots, a_{|A|}\}$ . Each attribute  $a_i$  may take  $|a_i|$  possible values. Let an entity  $e$  be described by particular realizations of  $A$ . Thus, an entity  $e_i$  can be written as an  $|A|$ -dimensional vector.

We define a context  $c$  as a lossless representation of  $N_c$  entities. Let  $q$  be one or more queries about the value of a particular attribute of an entity in  $c$ . Let  $y$  be the correct answer to queries in  $q$ .

Altogether, we can define  $\mathcal{D} = \{(c_i, q_i, y_i), i = 1..N\}$  to be a dataset of  $N$  samples, where  $c_i, q_i, y_i$  refer to the context, queries and answers for the  $i$ -th element in the dataset. The task consists of predicting the correct  $a_i$ , given  $c_i$  and  $q_i$ .

## 2.2. Evaluation

To perform our evaluation, as is standard in the systematic generalization literature, we will assume two latent attributes  $\{a, b \in A\}$ , where  $b$  is the attribute we wish to predict systematically. We will work with two data distributions; Split A: where properties  $a$  and  $b$  are related; and Split B, where this relation does not hold. Specifically, Split A will contain a subset of all combinations of  $a$  and  $b$ , while Split B will contain all remaining combinations. During our experiments, we use three different sets for training and evaluation: training ( $\mathcal{D}_{train}$ ), test in-distribution ( $\mathcal{D}_{test-ID}$ ), and test out-of-distribution ( $\mathcal{D}_{test-OOD}$ ).  $\mathcal{D}_{train}$  and  $\mathcal{D}_{test-ID}$  come from Split A, while  $\mathcal{D}_{test-OOD}$  comes from Split B. During evaluation we will focus on performance on property  $b$ .

## 2.3. Distributional Properties of Training Data

We wish to study how three properties of  $\mathcal{D}_{train}$  affect SG. Therefore, we look for distributional properties of  $\mathcal{D}_{train}$  that might be able to break the link between  $a$  and  $b$ . To achieve this, we propose three properties, give intuition on why they may work to achieve this goal, and define them.

### 2.3.1. Diversity

To disrupt the link between properties  $a$  and  $b$ , we propose to increase the total number of values  $a$  may take. Our hypothesis is that increasing the diversity of values of  $a$  on the training set might make it harder for the model to memorize all combinations of  $a$  and  $b$ . Thus, the model may prefer solutions that learn to detect  $a$  and  $b$  separately. Therefore, we propose *diversity over attribute  $a$*  as the total cardinality of  $a \in A$ , that is  $div(a) = |a_i|$ . Over our experiments, we modulate diversity over  $a$  in a dataset by altering the number of possible values  $a$  may take in the training set.

### 2.3.2. Burstiness

Another way to influence the link between  $a$  and  $b$  is to disrupt the learning of  $a$ , such that the model may not rely on  $a$  to predict  $b$ . To instantiate this idea as a data property, we propose the use of *burstiness*. *Burstiness over  $a$*  is defined as limiting the number of possible values  $a$  may take within an individual context  $c$ . Intuitively, this makes batches of data where only some value of  $a$  will be heavily featured, while on other batches a different set of values

for  $a$  will dominate. That is our intuition of *burstiness*. To modulate *burstiness*, we define a probability  $p_{burst}$  that a sample is bursty or not. This property is adapted for use in the MMLM setting from previous work [10], where it was applied by limiting the number of different class labels and eliciting a meta-learning algorithm.

### 2.3.3. Latent Intervention

Finally, another way to break this link is to directly alter the value of  $a$  while keeping the value of  $b$  constant. This approach is reminiscent of the Causal Inference literature [53, 54], which uses interventions over causal variables to learn interventional probability distributions, that is, the probability distribution of outcomes should a certain intervention be affected. Thus, *latent intervention of  $a$*  is related to altering the values of a latent attribute consistently across all entities in a context  $c$ . We modulate the degree of latent intervention by the amount the attribute is altered.

## 3. Experimental Setup

We proceed to detail how we operationalize the ideas from the previous section.

### 3.1. Dataset

We create a dataset resembling the structure of the CLEVR dataset [32] by leveraging their generative code. Attributes for this dataset are  $A = \{shape, color, material, size\}$ . Our main goal is to predict the *shape* attribute systematically, while excluding certain combinations of *shape-color* from  $\mathcal{D}_{train}$ . There are three possible shapes:  $\{sphere, cube, cylinder\}$ . The context for this dataset is a 224 x 224 color image of 3 to 10 objects. Queries are defined as a textual description of the scene where the property of the object that is to be predicted is masked. Contextual information is also included in the query to make queries unambiguous. Our training set consists of 75,000 samples and the test set of 15,000.

Properties  $a$  and  $b$  will be color and shape, respectively. We designate a subset of shapes (*cubes* and *cylinders*) to introduce systematic differences. That is, some combinations of these shapes and colors will be in Split A, while the rest will be in Split B. Spheres, on the other hand, will combine to all colors in every split, so they may act as a control.

### 3.2. Distributional Properties of the Training Data

We modulate diversity by altering the number of colors available in the  $\mathcal{D}_{train}$ . We test the following total number of colors:  $\{8, 27, 64, 125, 216\}$ . These values come from dividing the color span in each channel in  $n \in \{2..6\}$  equal parts. Burstiness is implemented by limiting the number of possible colors in a given image to 3. This property is modulated by altering  $p_{burst}$  with the following values:  $\{0.0, 0.5, 1.0\}$ . Finally, we implement latent intervention

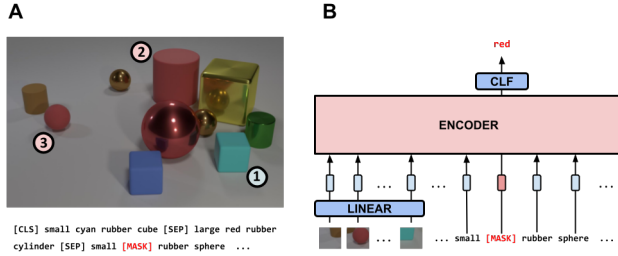


Figure 1. (A) Example input for our task. Image shows objects with different properties, while query gives a textual description of the objects, while masking properties to be predicted. Sample query lists numbered objects from 1-3. (B) Diagram of the model during training. Context is provided as an image, while the *query* consists of text denoting information about the scene with some text related to properties of objects are masked. Both the context and query are entered into a Transformer Encoder, where it classifies for each masked token the most probable value of the masked property in the query.

by randomly altering the hue of all colors in the image via the *ColorJitter* transform in PyTorch [50]. Our experiments use the following values:  $\{0.0, 0.05, 0.1, 0.5\}$ .

### 3.3. Model

We use a Transformer encoder [62] that receives both the context and query as inputs. Following standard procedure [15], images are divided into patches and arranged into a sequence of embeddings via a linear layer. The text is passed through an embedding layer. Learned positional and modality (image or text) embeddings are added to the input before the encoder. Both sequence embeddings are concatenated and fed into the transformer encoder (see Fig. 1).

### 3.4. Evaluation

We run each experiment for 3 seeds and report their mean and standard error. All metrics are related to performance on cubes and cylinders to correctly assess for generalization in objects with systematic differences to the training set.

## 4. Baseline Results on SG

We first analyze the behavior of a baseline model trained on 8-colors in  $\mathcal{D}_{train}$ , probing its ability to predict specific attributes. The results are shown in Fig. 2.

In-distribution performance remains similar to that of  $\mathcal{D}_{train}$  for all tasks. However, delving into performance for  $\mathcal{D}_{test-OOD}$  reveals three distinct generalization patterns. First, unexpectedly, the *material* and *size* show a decrease in  $\mathcal{D}_{test-OOD}$  performance, even though the model has been exposed to all combinations of these attributes during training. Second, we observe a significant decrease in performance for the *color* task (44% drop) and *shape* (99% drop). This is especially bad for the *shape* task which achieves

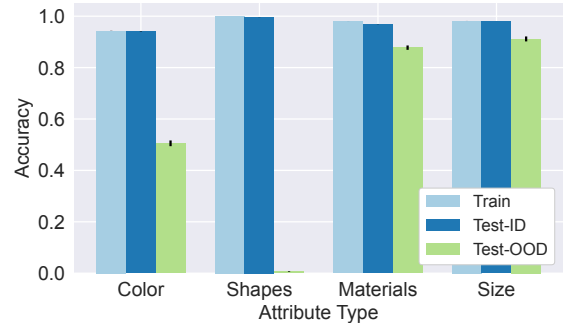


Figure 2. Accuracy for predicting different properties for different data splits for the baseline model (8 colors). In-distribution performance for all tasks remains high, however out-of-distribution performance plummets for *shape* and *color*, suggesting the model is learning combinations of *shape-color* as features, instead of achieving systematic generalization. Unexpectedly, material and size also show a drop in out-of-distribution performance, even though the model has been exposed to all combinations of these attributes in training.

much worse than random performance (33% to predict between three shapes in  $\mathcal{D}_{test-OOD}$ ). These results strongly suggest that the model faces challenges when performing SG. These results confirm previous findings that indicate DNNs encounter significant performance challenges when required to generalize systematically [33, 34, 37, 60]. Third, given that both shape and color are related systematically, a natural question arises: why is *color* less affected than *shape*? An explanation for this difference in performance between *color* and *shape* on  $\mathcal{D}_{test-OOD}$  emerges from how image information is fed to the model. Due to the division of images into patches, the model can predict the color of a particular object solely based on the information of one patch. However, to predict the shape of an object, the model needs information from additional patches, making this ability harder to train and thus successfully achieve SG.

We turn to analyzing how modulating the amount of training data affects SG. A popular way of promoting generalization is to increase the amount of training data. Therefore, we train models on different percentages of  $\mathcal{D}_{train}$ . Results are shown in Figure 3a. While in-distribution performance roughly stays the same, increasing the amount of training data does not result in better out-of-distribution generalization. Performance degrades as dataset size increases. This suggests that merely adding more in-distribution training data may not be a robust way of inducing a bias toward systematic generalization. Even worse, it seems to double down on whatever non-systematic bias the model is learning. We now alter the distribution of  $\mathcal{D}_{train}$ .

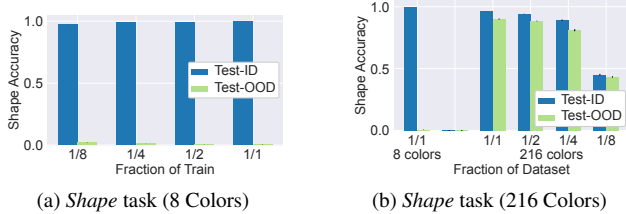


Figure 3. Accuracy for the *shape* task for different amounts of training data for the baseline model (8 colors) vs model trained on 216 colors. (a) Increasing dataset size does not increase out-of-distribution performance but rather degrades it slightly. (b) With increased *diversity* much stronger out-of-distribution generalization is achieved, with models trained on only a quarter of the data severely outperforming the 8-color baseline.

## 5. Impact of Altering the Training Distribution on SG

We investigate the impact on SG of altering  $\mathcal{D}_{train}$  by manipulating properties specifically tailored to perturbate the link between  $a$  and  $b$ .

### 5.1. Diversity

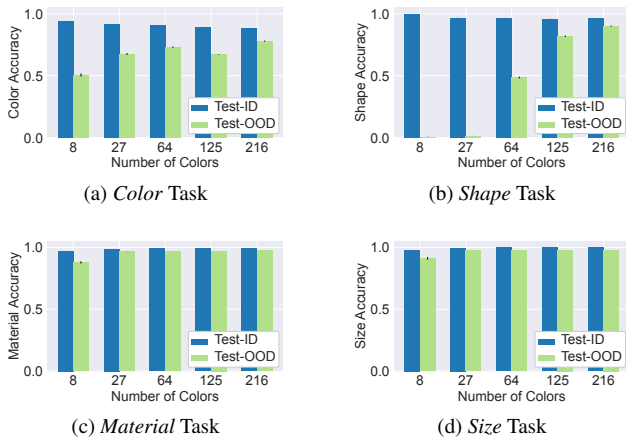


Figure 4. Accuracy versus the number of colors in  $\mathcal{D}_{train}$  for  $\mathcal{D}_{test-ID}$  and  $\mathcal{D}_{test-OOD}$  for the *color* and *shape* tasks. Performance for the *shape* task increases drastically for the OOD split as we increase colors, increasing 86% in absolute terms over the 8-color baseline. Moreover, performance in the color task also tends to increase in the out-of-distribution split, while in-distribution only suffers slightly, even though the task becomes significantly harder. Remarkably, the *material* and *size* task rapidly increase their  $\mathcal{D}_{test-OOD}$  performance as color increases.

To increase *diversity*, we run experiments where we increase colors in  $\mathcal{D}_{train}$  from 8 to 216. Figure 4 shows these results. We observe that augmenting *color diversity* improves SG on the *shape* task (see monotonic increase of **green bars**). This increase is of an absolute 89%, a stagger-

ing amount that reflects the difference between a model that does not generalize systematically to one that does. Unexpectedly, the performance on color prediction barely decreases in test-ID (around 6%) (Fig. 4a), in spite of the increased difficulty of the task given by a higher number of classes. Moreover, increased color diversity reduces the performance gap between  $\mathcal{D}_{test-ID}$  and  $\mathcal{D}_{test-OOD}$  in the *color* task (Fig. 4a). Remarkably, out-of-distribution performance for the *material* and *size* tasks also increases significantly when augmenting colors. This suggests that increased diversity seems to be creating an inductive bias where at least *color* is being disassociated from *shape*, *material* and *size*. Moreover, this increase for *material* and *size* occurs rapidly with just 27 colors, while for *shape* this keeps increasing until reaching 216 colors.

Finally, we test whether increasing diversity affects the model’s sample efficiency. We proceed to train models on datasets with 216 colors with size  $\{0.25, 0.5, 0.75\}$  of the original training size and compare them to the 8-color baseline at full training size. Results are shown in Figure 3b. As can be seen, even training with just one quarter of the original training size with increased diversity produces much stronger out-of-distribution generalization than the baseline, while the gap between in-distribution and out-of-distribution remains relatively low.

### 5.2. Burstiness

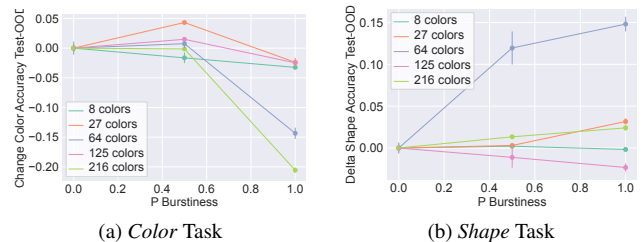


Figure 5. Change of accuracy with respect to no burstiness for the *color* and *shape* tasks in test-ID and test-OOD for different levels of *burstiness* over *color* for various numbers of colors. Limiting the number of colors available for each image during training allows the model to gain up to 14.8% more accuracy over the baseline. The *color* task, however, suffers up to 14.3% decline as the *color* task becomes easier to memorize.

As was mentioned in Section 2.3, another way of disrupting the link between *color* and *shape*, is to hinder the learning of *color* by limiting the number of colors contained in a given image, something we call *burstiness*. Figure 5 shows the results. As can be seen, increasing the *burstiness* of the training data increases the SG capability of the model in the *shape* task by up to 14.8%. As expected, however, the *color* task is significantly affected, both in  $\mathcal{D}_{test-ID}$  and  $\mathcal{D}_{test-OOD}$ , losing up to 14.3% accuracy in  $\mathcal{D}_{test-OOD}$  for 64 colors. This last effect is especially pronounced as we in-

crease the number of colors contained in the dataset, which is to be expected as the *color* task becomes significantly harder as the number of colors increases dramatically, while the limit of only 3 colors per image remains fixed. Finally, the effect of *burstiness* on *material* and *size* is very small, with at most 1% gain in  $\mathcal{D}_{test-OOD}$ .

### 5.3. Latent Intervention

Figure 6 shows results for modulating *latent intervention* over *color*. In our experiments, we can observe that increasing the degree of the perturbation we apply to the color of the images during training increases the model performance on the *shape* task by up to 15%, a non-trivial amount while retaining out-of-distribution performance on the *color* task. For the *material* and *size* tasks, latent intervention adds up to 2% in  $\mathcal{D}_{test-OOD}$  performance, and the effect is reduced as the number of colors increases.

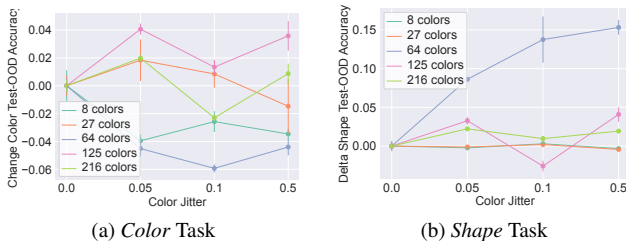


Figure 6. Change in accuracy after applying latent intervention for the *color* and *shape* tasks in test-ID and test-OOD for different levels of latent intervention of the *color* latent attribute for various numbers of colors. X-Axis not at scale. Altering the color hue randomly during training allows the model to gain up to 15% more out-of-distribution accuracy over baseline.

### 5.4. Discussion

While all properties improve SG in the *shape* task, *diversity* clearly seems to have the greatest impact overall. However, we see that the other properties seem to be complementary to diversity. This suggests a positive answer to our research question “*Can Systematic Generalization be induced solely through changing properties of the training data?*”.

Surprisingly, the effects of altering these properties does not only affect performance in  $\mathcal{D}_{test-OOD}$  for *shape* and *color*, but also *material* and *size*. This suggests that by default a model will tend to combine all latent features in the representation. We show that by especially targeting the spurious relation between latent factors through changes of the training distribution, this model behavior can be altered. We showed three ways in which this could be done with differing levels of success. This answers our second question: “*How can we alter the training distribution to unduce SG?*”. Finally, we move to answer why these properties affect SG. To do that, we will first study model capacity for SG.

## 6. Lack of Capacity does not explain SG

Given that *diversity* has shown to improve SG performance, we would like to gain a deeper understanding of why this is the case. Our first hypothesis is the following: adding more colors to the training distribution strains the capacity of the model such that it is forced to learn simpler learning solutions *shape* and *color* independently of each other. In other words, lack of capacity may force the model to find a more systematic solution. To test this, we test two cases: 1) We artificially restrict the capacity of a baseline Transformer model trained on 8 colors by limiting the size of the residual stream dimension ( $d \in \{32, 64, 128\}$ ). 2) We augment the capacity of the model trained on 216 colors by increasing this dimension by  $\{512, 1024\}$ .

Figure 7 shows results for these experiments. As can be seen, performance in both  $\mathcal{D}_{test-ID}$  and  $\mathcal{D}_{test-OOD}$  decreases as model capacity is reduced in the first case, and the converse happens when we increase capacity. So, lack of capacity does not seem to be the mechanism by which *diversity* achieves SG. We now turn to mutual information between latent attributes as a possible explanation.

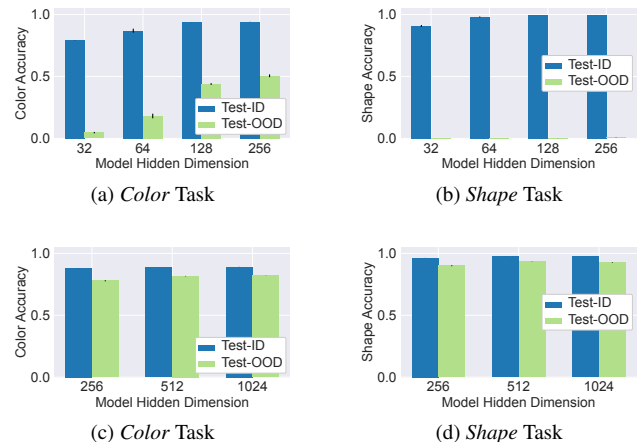


Figure 7. In-Distribution and Out-of-Distribution accuracy for models trained with different values for their hidden dimensions on a training set with 216 colors for the *color* and *shape* task. (a-b) When exposed to low diversity (8 colors) both metrics suffer as model capacity is reduced. (c-d) Both metrics increase as model capacity is increased. These results suggest that lack of capacity of the models is not the cause for achieving greater SG when augmenting the number of colors in the training set.

## 7. Mutual Information versus Diversity

Previous work [1] has shown that there is a relation between the Normalized Mutual Information (NMI) of latent attributes and systematic generalization. Mutual information quantifies the amount of information one variable (e.g., *shape*) provides about another (e.g., *color*). Then, this value

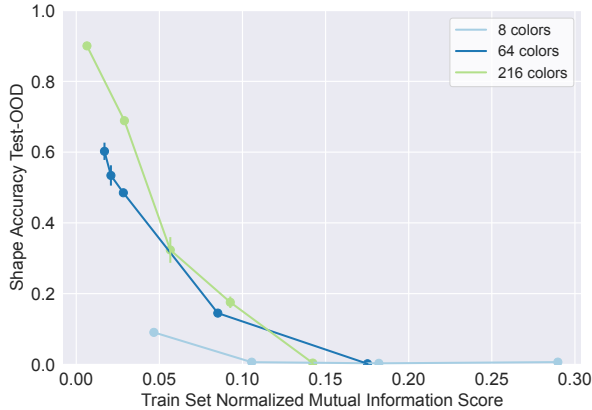


Figure 8. Normalized Mutual Information in the Training Set vs Out-of-Distribution Accuracy for the *shape* task for datasets with 8, 64 and 216 colors. For lower NMI, there is greater out-of-distribution performance. However, for similar levels of NMI but differing levels of *diversity*, we observe that greater *diversity* increases performance. This suggests that the effect of *diversity* is not only related to changing the NMI in the dataset.

is normalized with the entropy of the distributions to produce the NMI. The closer NMI is to zero, the more independent these factors are. In other words, a near-zero mutual information score indicates that the dataset offers strong evidence to the model that *shape* and *color* should be treated as independent attributes.

Changing *diversity* in a dataset impacts its NMI, so we proceed to study this effect. We seek to decouple the effect of increased *diversity* from a dataset’s NMI. To modulate NMI for a given level of *diversity*, we produce datasets that assign colors that both *cubes* and *cylinders* see during training (common colors) and a set of colors that are only seen either by *cubes* or by *cylinders* (exclusive colors). Modulating the ratio of common colors within the dataset directly alters its NMI, while keeping the total number of colors constant.

To measure the NMI, we follow previous work [1] and focus on the NMI between the *color* and *shape* of all objects of the training dataset. It shows a Pearson correlation of  $-0.79$ . Figure 8 plots results for datasets with differing levels of *diversity*. For lower NMI, there is greater out-of-distribution performance. However, for similar levels of NMI but differing levels of *diversity*, we observe that greater *diversity* increases performance. This suggests that the effect of *diversity* is not only related to changing the NMI in the dataset but rather other properties. Finally, we study the geometry of representations induced by *diversity*.

## 8. Geometry of Representations

### 8.1. Disentanglement

A desirable property for SG is disentangled representations [17, 27, 28]. Using DCI metrics [19], we focus on measures of Disentanglement and Completeness. *Disentanglement* measures how many latent attributes each dimension of the representation can predict. A score of 0 implies that each dimension has an equal predictive power for all latent attributes, while a score of 1 suggests that each dimension exclusively predicts a single latent attribute. *Completeness* measures the extent to which different dimensions of the representation predict each latent attribute. A score of 0 means each latent attribute is predicted equally by all dimensions, whereas a score of 1 indicates that only one dimension is responsible for predicting each latent attribute.

Figure 9 shows results for these metrics for representations for the *color* and *shape* task derived from models with different levels of *color diversity*. Increased diversity for *shape* task representations leads to both greater disentanglement and completeness, while the converse is true for *color* task representations.

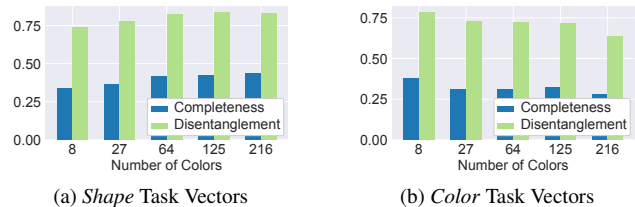


Figure 9. Disentanglement and Completeness for models trained on different levels of *color diversity* for vectors predicting the *shape* and *color* tasks. Both disentanglement and completeness increase for the *shape* task vectors, while the contrary happens for *color* task vectors.

We also complement our analysis by drawing from neuroscience-inspired studies that have demonstrated the potential of parallelism in representations for enhancing generalization [8, 30].

### 8.2. Parallelism in Representations

The intuition behind studying parallelism in representations is that two objects with a single different factor should have a constant direction offset in their representation, independent of other factors or context. Thus, that factor is encoded in representational space as the direction of the difference between both objects’ representations.

For instance, think on a classic example for analogy in DNNs:  $king - man + woman = queen$  which implies:  $king - man = queen - woman = royalness$ .

In this case, subtracting the abstract concept of gender gives us vectors that move in the same direction (an abstract

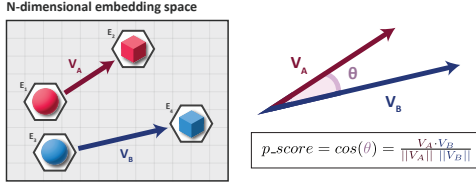


Figure 10. Computation of the  $p$ -score metric for vectors  $V_A$  and  $V_B$ , representing the effect of ablating features on *shape* embeddings. We first subtract the embeddings to obtain vectors  $V_A$  and  $V_B$  and then calculate the degree of parallelism between them using cosine distance. A high  $p$ -score indicates strong parallelism, suggesting that the attribute (in this case, *cubeness*) is encoded consistently in representational space.

property one might consider *royalness*) for two otherwise different vectors. Encoding this property consistently in a single direction allows the model to generalize that concept by way of *analogy*. Analogy is a powerful inductive bias for solving new tasks [47].

We proceed to apply this same principle to the latent factors contained in our dataset. From a starting set of 1.024 images, we sample 3.500 pairs of representations from objects that share a common latent attribute. To represent each object we use the representation vector associated to the attribute we wish to study, which in this case will be either *shape* or *color*. We proceed to find for each of these pairs another pair of representations which represents a change in this attribute (i.e. for *shape*, from a pair of red and green cubes, we look for a pair of red and green cylinders). We subtract these pairs and from the resulting pair we obtain a single value called a  $p$ -score [30]. This score is calculated by measuring the cosine of the angle between vectors in the resulting pair. We report the mean of this value over the 3.500 pairs averaged over 5 runs.

We relate the  $p$ -score with performance on  $\mathcal{D}_{test-ODD}$  for both the *shape* and *color* task for all models mentioned in Sections 4 and 5. Results for experiments with 8, 64, and 216 colors are shown in Figure 11a. Relating to the generalization capabilities in the *shape* task, we see a positive trend in o.o.d generalization when the  $p$ -score increases.

To understand how significant this relationship is, we calculate the Pearson correlation between  $p$ -score and out of distribution performance on the *shape* task. See supplementary material for details. We obtain a 0.73 Pearson correlation with very low p-value, suggesting the strong relationship between  $p$ -score and SG.

We also plot the relationship between NMI and  $p$ -score, as the positive relation both values have out-of-distribution generalization might be mediated by one or the other. Results are shown in Figure 11b. A clear relationship between NMI and  $p$ -score appears: lower NMI datasets are related to higher  $p$ -scores in representations. Given that

NMI is a stable property of the dataset, this suggests that lower NMI datasets tend to produce models with representations with higher p-scores. This suggests a novel mechanism by which lower NMI datasets produce inductive biases during learning that allow models to achieve greater out-of-distribution generalization. These results provide evidence that the *dataset distribution influences the representational space geometry of the model* biasing it towards out-of-distributional generalization.

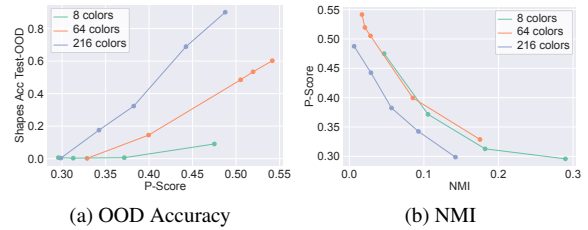


Figure 11. (a) Out-of-distribution accuracy versus  $p$ -score for models trained on 8, 64 and 216 colors for both the *shape* task. A trend can be seen that increasing performance is related to higher parallelism scores in the representation. (b) NMI vs  $p$ -score for various models. Lower NMI datasets produce models with representations with higher  $p$ -score suggesting a mechanism by which lower NMI aids in achieving SG.

## 9. Related Work

**Systematic Generalization.** Many works have addressed the problem of SG, proposing a variety of strategies. These include data augmentation methods [2–4, 64], training methods [11, 38, 39], adjustments to the loss function [26], architectural changes [5, 13, 18, 22, 36, 49, 56] and neuro-symbolic approaches [44, 48]. Currently, state-of-the-art methods are based on enhanced LLMs [16, 57].

**Data-driven Inductive Biases.** Previous work has investigated the invariances [9], inductive biases such as shape bias [23], and robustness [20] acquired by deep learning models when trained on large-scale datasets. Prystawski et al. [55] shows the need for local structure in the training data for models to learn probabilistic reasoning abilities.

Other studies have examined the data properties that enable models to generalize OOD. Chan et al. [10] show that burstiness, long-tailed distributions and label mappings can foster in-context learning in Transformers. By contrast, our work focuses specifically on data properties that support SG. For SG, studies have shown that increasing the number of primitives or input length can enhance SG [52, 58, 65]. However, their focus is on generalization in the text domain, while we focus on images, examining how different latent factors within the dataset interact to drive SG.

Other work on generalization in the visual domain [1] has investigated SG in CLIP models, showing that statisti-

cal independence between object-attribute pairs and disentangled representations enhances SG. In contrast, we analyze the effects of explicit generative factors on SG and the mechanisms by which it is enforced.

## 10. Conclusion

We advocate for a different way of creating inductive biases for SG on our models, by focusing on *altering the training distribution* over other techniques. We show three ways of manipulating the training distribution that provide significant increases in systematic generalization: *diversity*, *burstiness* and *latent intervention*. All of these properties enhance SG significantly, with *diversity* being the most important, enhancing up to an absolute 89% over the baseline, while the rest seem to be complementary to diversity.

We also study why these are effective. We show that limiting model capacity is not a factor for SG, while increased disentanglement and lower NMI between latent attributes in the dataset seem to explain most of the gains in SG. Crucially, we test for a property of brain-like representations which measures parallelism in representations under changes in a latent attribute. We find that datasets with lower NMI tend to induce more of this parallelism, a property that allows models to extrapolate by analogy. This is, to the best of our knowledge, an unreported mechanism by which dataset distribution induces SG.

## Acknowledgements

This work was supported by FONDECYT under Grant 1221425; and National Center for Artificial Intelligence (CENIA) under Grant FB210017 Basal ANID.

## References

- [1] Reza Abbasi, Mohammad Hossein Rohban, and Mahdieh Soleymani Baghshah. Deciphering the role of representation disentanglement: Investigating compositional generalization in clip models, 2024. 2, 6, 7, 8
- [2] Ekin Akyurek and Jacob Andreas. LexSym: Compositionality as lexical symmetry. In *Proceedings of the 61st Annual Meeting of the Association for Computational Linguistics (Volume 1: Long Papers)*, pages 639–657, Toronto, Canada, 2023. Association for Computational Linguistics. 8
- [3] Ekin Akyürek, Afra Feyza Akyürek, and Jacob Andreas. Learning to recombine and resample data for compositional generalization. In *International Conference on Learning Representations*.
- [4] Jacob Andreas. Good-enough compositional data augmentation. In *Proceedings of the 58th Annual Meeting of the Association for Computational Linguistics*, pages 7556–7566, 2020. 8
- [5] Dzmitry Bahdanau, Shikhar Murty, Michael Noukhovitch, Thien Huu Nguyen, Harm de Vries, and Aaron Courville. Systematic generalization: What is required and can it be learned? In *International Conference on Learning Representations*, 2019. 8
- [6] Hangbo Bao, Wenhui Wang, Li Dong, Qiang Liu, Owais Khan Mohammed, Kriti Aggarwal, Subhojit Som, Songhao Piao, and Furu Wei. Vlm0: Unified vision-language pre-training with mixture-of-modality-experts. *Advances in Neural Information Processing Systems*, 35:32897–32912, 2022. 2
- [7] Jonathan Baxter. A model of inductive bias learning. *Journal of artificial intelligence research*, 12:149–198, 2000. 2
- [8] Silvia Bernardi, Marcus K Benna, Mattia Rigotti, Jérôme Munuera, Stefano Fusi, and C Daniel Salzman. The geometry of abstraction in the hippocampus and prefrontal cortex. *Cell*, 183(4):954–967, 2020. 7
- [9] Diane Bouchacourt, Mark Ibrahim, and Ari Morcos. Grounding inductive biases in natural images: invariance stems from variations in data. *Advances in Neural Information Processing Systems*, 34:19566–19579, 2021. 2, 8
- [10] Stephanie Chan, Adam Santoro, Andrew Lampinen, Jane Wang, Aaditya Singh, Pierre Richemond, James McClelland, and Felix Hill. Data distributional properties drive emergent in-context learning in transformers. *Advances in Neural Information Processing Systems*, 35:18878–18891, 2022. 3, 8
- [11] Henry Conklin, Bailin Wang, Kenny Smith, and Ivan Titov. Meta-learning to compositionally generalize. In *Proceedings of the 59th Annual Meeting of the Association for Computational Linguistics and the 11th International Joint Conference on Natural Language Processing (Volume 1: Long Papers)*, pages 3322–3335, 2021. 8
- [12] Ronald B Dekker, Fabian Otto, and Christopher Summerfield. Curriculum learning for human compositional generalization. *Proceedings of the National Academy of Sciences*, 119(41):e2205582119, 2022. 1
- [13] Roberto Dessì and Marco Baroni. Cnns found to jump around more skillfully than rnns: Compositional generalization in seq2seq convolutional networks. In *Proceedings of the 57th Annual Meeting of the Association for Computational Linguistics*, pages 3919–3923, 2019. 8
- [14] Jacob Devlin, Ming-Wei Chang, Kenton Lee, and Kristina Toutanova. BERT: Pre-training of deep bidirectional transformers for language understanding. In *Proceedings of the 2019 Conference of the North American Chapter of the Association for Computational Linguistics: Human Language Technologies, Volume 1 (Long and Short Papers)*, pages 4171–4186, Minneapolis, Minnesota, 2019. Association for Computational Linguistics. 2
- [15] Alexey Dosovitskiy, Lucas Beyer, Alexander Kolesnikov, Dirk Weissenborn, Xiaohua Zhai, Thomas Unterthiner, Mostafa Dehghani, Matthias Minderer, Georg Heigold, Sylvain Gelly, et al. An image is worth 16x16 words: Transformers for image recognition at scale. In *International Conference on Learning Representations*, 2020. 4
- [16] Andrew Drozdov, Nathanael Schärli, Ekin Akyürek, Nathan Scales, Xinying Song, Xinyun Chen, Olivier Bousquet, and Denny Zhou. Compositional semantic parsing with large lan-

- guage models. In *The Eleventh International Conference on Learning Representations*. 8
- [17] Sunny Duan, Loic Matthey, Andre Saraiva, Nick Watters, Chris Burgess, Alexander Lerchner, and Irina Higgins. Un-supervised model selection for variational disentangled representation learning. In *International Conference on Learning Representations*, 2020. 7
- [18] Yann Dubois, Gautier Dagan, Dieuwke Hupkes, and Elia Bruni. Location attention for extrapolation to longer sequences. In *Proceedings of the 58th Annual Meeting of the Association for Computational Linguistics*, pages 403–413, 2020. 8
- [19] Cian Eastwood and Christopher K. I. Williams. A framework for the quantitative evaluation of disentangled representations. In *International Conference on Learning Representations*, 2018. 7
- [20] Alex Fang, Gabriel Ilharco, Mitchell Wortsman, Yuhao Wan, Vaishal Shankar, Achal Dave, and Ludwig Schmidt. Data Determines Distributional Robustness in Contrastive Language Image Pre-training (CLIP). In *Proceedings of the 39th International Conference on Machine Learning*, pages 6216–6234. PMLR, 2022. 2, 8
- [21] Jerry A Fodor. *The language of thought*. Harvard university press, 1975. 1
- [22] Tong Gao, Qi Huang, and Raymond Mooney. Systematic generalization on gSCAN with language conditioned embedding. In *Proceedings of the 1st Conference of the Asia-Pacific Chapter of the Association for Computational Linguistics and the 10th International Joint Conference on Natural Language Processing*, pages 491–503, Suzhou, China, 2020. Association for Computational Linguistics. 8
- [23] Robert Geirhos, Patricia Rubisch, Claudio Michaelis, Matthias Bethge, Felix A. Wichmann, and Wieland Brendel. Imagenet-trained CNNs are biased towards texture; increasing shape bias improves accuracy and robustness. In *International Conference on Learning Representations*, 2019. 1, 8
- [24] Anirudh Goyal and Yoshua Bengio. Inductive biases for deep learning of higher-level cognition. *Proceedings of the Royal Society A*, 478(2266):20210068, 2022. 2
- [25] Susan A Graham and Diane Poulin-Dubois. Infants’ reliance on shape to generalize novel labels to animate and inanimate objects. *Journal of child language*, 26(2):295–320, 1999. 1
- [26] Christina Heinze-Deml and Diane Bouchacourt. Think before you act: A simple baseline for compositional generalization. 2020. 8
- [27] Irina Higgins, Loic Matthey, Arka Pal, Christopher Burgess, Xavier Glorot, Matthew Botvinick, Shakir Mohamed, and Alexander Lerchner. beta-VAE: Learning basic visual concepts with a constrained variational framework. In *International Conference on Learning Representations*, 2017. 7
- [28] Irina Higgins, David Amos, David Pfau, Sebastien Racaniere, Loic Matthey, Danilo Rezende, and Alexander Lerchner. Towards a definition of disentangled representations, 2018. 7
- [29] Takuya Ito, Tim Klinger, Doug Schultz, John Murray, Michael Cole, and Mattia Rigotti. Compositional generalization through abstract representations in human and artificial neural networks. *Advances in Neural Information Processing Systems*, 35:32225–32239, 2022. 2
- [30] Takuya Ito, Tim Klinger, Doug Schultz, John Murray, Michael Cole, and Mattia Rigotti. Compositional generalization through abstract representations in human and artificial neural networks. *Advances in neural information processing systems*, 35:32225–32239, 2022. 7, 8
- [31] Yichen Jiang, Xiang Zhou, and Mohit Bansal. Mutual exclusivity training and primitive augmentation to induce compositionality. In *Proceedings of the 2022 Conference on Empirical Methods in Natural Language Processing*, pages 11778–11793, Abu Dhabi, United Arab Emirates, 2022. Association for Computational Linguistics. 2
- [32] Justin Johnson, Bharath Hariharan, Laurens Van Der Maaten, Li Fei-Fei, C Lawrence Zitnick, and Ross Girshick. Clevr: A diagnostic dataset for compositional language and elementary visual reasoning. In *Proceedings of the IEEE conference on computer vision and pattern recognition*, pages 2901–2910, 2017. 2, 3
- [33] Daniel Keysers, Nathanael Schärli, Nathan Scales, Hylke Buisman, Daniel Furrer, Sergii Kashubin, Nikola Momchev, Danila Sinopalnikov, Lukasz Stafiniak, Tibor Tihon, et al. Measuring compositional generalization: A comprehensive method on realistic data. In *International Conference on Learning Representations*, 2019. 1, 4
- [34] Najoung Kim and Tal Linzen. Cogs: A compositional generalization challenge based on semantic interpretation. In *Proceedings of the 2020 Conference on Empirical Methods in Natural Language Processing (EMNLP)*, pages 9087–9105, 2020. 1, 4
- [35] Jan Kukačka, Vladimir Golkov, and Daniel Cremers. Regularization for deep learning: A taxonomy. *arXiv preprint arXiv:1710.10686*, 2017. 2
- [36] Yen-Ling Kuo, Boris Katz, and Andrei Barbu. Compositional networks enable systematic generalization for grounded language understanding. *arXiv preprint arXiv:2008.02742*, 2020. 8
- [37] Brenden Lake and Marco Baroni. Generalization without systematicity: On the compositional skills of sequence-to-sequence recurrent networks. In *International conference on machine learning*, pages 2873–2882. PMLR, 2018. 1, 4
- [38] Brenden M Lake. Compositional generalization through meta sequence-to-sequence learning. In *Advances in Neural Information Processing Systems 32*, pages 9791–9801. Curran Associates, Inc., 2019. 2, 8
- [39] Brenden M Lake and Marco Baroni. Human-like systematic generalization through a meta-learning neural network. *Nature*, 623(7985):115–121, 2023. 2, 8
- [40] Brenden M Lake, Tomer D Ullman, Joshua B Tenenbaum, and Samuel J Gershman. Building machines that learn and think like people. *Behavioral and brain sciences*, 40:e253, 2017. 1
- [41] Junnan Li, Dongxu Li, Caiming Xiong, and Steven Hoi. Blip: Bootstrapping language-image pre-training for unified vision-language understanding and generation. In *International conference on machine learning*, pages 12888–12900. PMLR, 2022. 2

- [42] Junnan Li, Dongxu Li, Silvio Savarese, and Steven Hoi. Blip-2: Bootstrapping language-image pre-training with frozen image encoders and large language models. In *International conference on machine learning*, pages 19730–19742. PMLR, 2023.
- [43] Xiujun Li, Xi Yin, Chunyuan Li, Pengchuan Zhang, Xiaowei Hu, Lei Zhang, Lijuan Wang, Houdong Hu, Li Dong, Furu Wei, et al. Oscar: Object-semantics aligned pre-training for vision-language tasks. In *Computer Vision–ECCV 2020: 16th European Conference, Glasgow, UK, August 23–28, 2020, Proceedings, Part XXX 16*, pages 121–137. Springer, 2020. 2
- [44] Qian Liu, Shengnan An, Jian-Guang Lou, Bei Chen, Zeqi Lin, Yan Gao, Bin Zhou, Nanning Zheng, and Dongmei Zhang. Compositional generalization by learning analytical expressions. *Advances in Neural Information Processing Systems*, 33:11416–11427, 2020. 8
- [45] Jonathan Long, Evan Shelhamer, and Trevor Darrell. Fully convolutional networks for semantic segmentation. In *Proceedings of the IEEE conference on computer vision and pattern recognition*, pages 3431–3440, 2015. 2
- [46] Gary F Marcus. *The algebraic mind: Integrating connectionism and cognitive science*. MIT press, 2003. 1
- [47] Melanie Mitchell. Abstraction and analogy-making in artificial intelligence. *Annals of the New York Academy of Sciences*, 1505(1):79–101, 2021. 8
- [48] Maxwell I Nye, Armando Solar-Lezama, Joshua B Tenenbaum, and Brenden M Lake. Learning compositional rules via neural program synthesis. *arXiv preprint arXiv:2003.05562*, 2020. 8
- [49] Santiago Ontanón, Joshua Ainslie, Vaclav Cvicek, and Zachary Fisher. Making transformers solve compositional tasks. *arXiv preprint arXiv:2108.04378*, 2021. 8
- [50] Adam Paszke, Sam Gross, Francisco Massa, Adam Lerer, James Bradbury, Gregory Chanan, Trevor Killeen, Zeming Lin, Natalia Gimelshein, Luca Antiga, Alban Desmaison, Andreas Kopf, Edward Yang, Zachary DeVito, Martin Raison, Alykhan Tejani, Sasank Chilamkurthy, Benoit Steiner, Lu Fang, Junjie Bai, and Soumith Chintala. Pytorch: An imperative style, high-performance deep learning library. In *Advances in Neural Information Processing Systems 32*, pages 8024–8035. Curran Associates, Inc., 2019. 4
- [51] Arkil Patel, Satwik Bhattamishra, Phil Blunsom, and Navin Goyal. Revisiting the compositional generalization abilities of neural sequence models. In *Proceedings of the 60th Annual Meeting of the Association for Computational Linguistics (Volume 2: Short Papers)*, pages 424–434, Dublin, Ireland, 2022. Association for Computational Linguistics. 2
- [52] Arkil Patel, Satwik Bhattamishra, Phil Blunsom, and Navin Goyal. Revisiting the compositional generalization abilities of neural sequence models. In *Proceedings of the 60th Annual Meeting of the Association for Computational Linguistics (Volume 2: Short Papers)*, pages 424–434, 2022. 8
- [53] Judea Pearl. *Causality: Models, Reasoning and Inference*. Cambridge University Press, USA, 2nd edition, 2009. 3
- [54] Jonas Peters, Peter Bühlmann, and Nicolai Meinshausen. Causal Inference by using Invariant Prediction: Identification and Confidence Intervals. *Journal of the Royal Statistical Society Series B: Statistical Methodology*, 78(5):947–1012, 2016. 3
- [55] Ben Prystawski, Michael Li, and Noah Goodman. Why think step by step? reasoning emerges from the locality of experience. *Advances in Neural Information Processing Systems*, 36, 2024. 8
- [56] Linlu Qiu, Hexiang Hu, Bowen Zhang, Peter Shaw, and Fei Sha. Systematic generalization on gscan: What is nearly solved and what is next? In *Proceedings of the 2021 Conference on Empirical Methods in Natural Language Processing*, pages 2180–2188, 2021. 8
- [57] Linlu Qiu, Peter Shaw, Panupong Pasupat, Pawel Nowak, Tal Linzen, Fei Sha, and Kristina Toutanova. Improving compositional generalization with latent structure and data augmentation. In *Proceedings of the 2022 Conference of the North American Chapter of the Association for Computational Linguistics: Human Language Technologies*, pages 4341–4362, 2022. 8
- [58] Amir Rahimi, Vanessa D’Amario, Moyuru Yamada, Kentaro Takemoto, Tomotake Sasaki, and Xavier Boix. D3: Data diversity design for systematic generalization in visual question answering. *Transactions on Machine Learning Research*, 2024. 8
- [59] Siamak Ravanbakhsh, Jeff Schneider, and Barnabas Poczos. Equivariance through parameter-sharing. In *International conference on machine learning*, pages 2892–2901. PMLR, 2017. 2
- [60] Laura Ruis, Jacob Andreas, Marco Baroni, Diane Bouchacourt, and Brenden M Lake. A benchmark for systematic generalization in grounded language understanding. *Advances in Neural Information Processing Systems*, 33, 2020. 1, 4
- [61] Victor Garcia Satorras, Emiel Hoogeboom, and Max Welling. E (n) equivariant graph neural networks. In *International conference on machine learning*, pages 9323–9332. PMLR, 2021. 2
- [62] Ashish Vaswani, Noam Shazeer, Niki Parmar, Jakob Uszkoreit, Llion Jones, Aidan N Gomez, Łukasz Kaiser, and Illia Polosukhin. Attention is all you need. In *Advances in neural information processing systems*, pages 5998–6008, 2017. 4
- [63] David H Wolpert, William G Macready, et al. No free lunch theorems for search. Technical report, Citeseer, 1995. 2
- [64] Jingfeng Yang, Le Zhang, and Diyi Yang. Subs: Subtree substitution for compositional semantic parsing. In *Proceedings of the 2022 Conference of the North American Chapter of the Association for Computational Linguistics: Human Language Technologies*, pages 169–174, 2022. 8
- [65] Xiang Zhou, Yichen Jiang, and Mohit Bansal. Data factors for better compositional generalization. In *Proceedings of the 2023 Conference on Empirical Methods in Natural Language Processing*, pages 14549–14566, Singapore, 2023. Association for Computational Linguistics. 2, 8

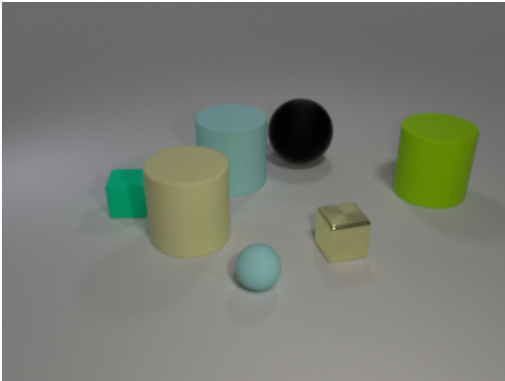
# Data Distributional Properties As Inductive Bias for Systematic Generalization

## Supplementary Material

### 11. Dataset Samples

Below we display samples composed of images and their corresponding textual descriptions from the datasets described in Section 3.1:

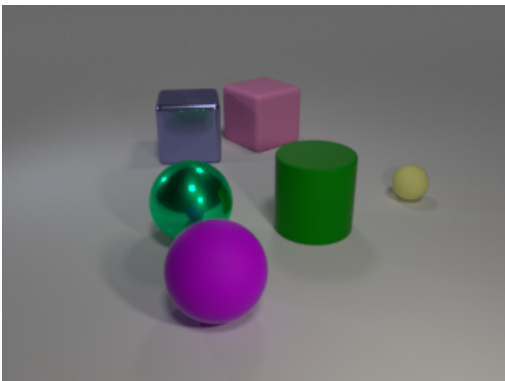
#### Sample 1



#### Textual Description

```
small #00ff80 rubber cube [SEP] large  
#ffff80 rubber cylinder [SEP] large #80ffff  
rubber cylinder [SEP] small #ffff80 metal  
cube [SEP] large #000000 rubber sphere  
[SEP] small #80ffff rubber sphere [SEP]  
large #80ff00 rubber cylinder
```

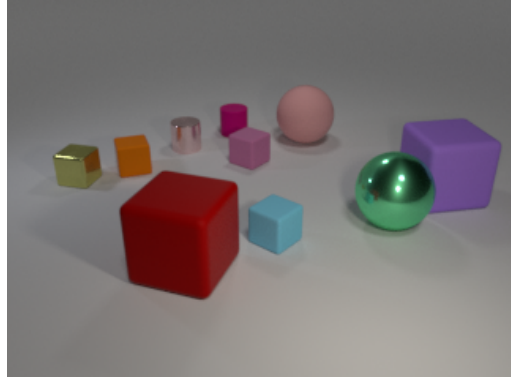
#### Sample 2



#### Textual Description

```
large #005500 rubber cylinder [SEP] large  
#5555aa metal cube [SEP] large #ff55aa  
rubber cube [SEP] small #ffff55 rubber  
sphere [SEP] large #aa00ff rubber sphere  
[SEP] large #00ff55 metal sphere
```

#### Sample 3



#### Textual Description

```
small #bf0040 rubber cylinder [SEP] large  
#40ff80 metal sphere [SEP] large #8040ff  
rubber cube [SEP] large #800000 rubber cube  
[SEP] small #bf4080 rubber cube [SEP] small  
#ffbfbf metal cylinder [SEP] small #ff4000  
rubber cube [SEP] small #40bfff rubber cube  
[SEP] small #bfbf40 metal cube [SEP] large  
#ff8080 rubber sphere
```

### 12. Correlation between P-Score and OOD Performance

In Table 1 we show the Pearson correlation between different p-scores obtained for a model and their OOD performance on the shape task. Parallelism in the representations seems to strongly correlate with better OOD performance, suggesting that parallelism may be the property that is inducing systematic generalization in the models.

METRIC	AVG	DIV	BURST	LI
CORR	0.73	0.76	0.69	0.73
P-VALUE	$1.88e-9$	$7.17e-4$	$5.5e-3$	$3.45e-5$

Table 1. Pearson Correlation between P-Scores and out-of-distribution performance on the *shape* task broken down per training data property. DIV: Diversity, BURST: Burstiness, LI: Latent Intervention.

### 13. Detailed Experimental Results

In tables 2, 3, 4, 5, 6, and 7, we exposed the values obtained that were used to generate most of the figures in the work above. Table 2 shows the data used for Figure 2. Table 3 for Figure 3. Table 4 for Figure 4. Table 5 for Figure 6. Table 6 for Figure 5. And, Table 7 for Figure 7.

	Train	Test-ID	Test-OOD
Color	94.3 ± 0.0%	94.1 ± 0.1%	50.5 ± 1.1%
Shapes	100.0 ± 0.0%	99.6 ± 0.0%	0.6 ± 0.1%
Materials	98.0 ± 0.0%	96.9 ± 0.0%	87.8 ± 0.9%
Size	98.1 ± 0.0%	98.0 ± 0.0%	91.2 ± 1.0%

Table 2. Table displaying values to form Figure 2. Accuracy for predicting different properties for different data splits for the baseline model (8 colors). In-distribution performance for all tasks remains high, however out-of-distribution performance plummets for shape and color, suggesting the model is learning combinations of shape-color as features, instead of achieving systematic generalization. Unexpectedly, material and size also show a drop in out-of-distribution performance, even though the model has been exposed to all combinations of these attributes in training.

Train Fract.	Color		Shape	
	Test-ID	Test-OOD	Test-ID	Test-OOD
8 Colors				
1/8	91.5 ± 0.1%	47.4 ± 0.4%	97.1 ± 0.1%	2.1 ± 0.1%
1/4	93.1 ± 0.1%	47.4 ± 0.5%	99.0 ± 0.0%	1.2 ± 0.1%
1/2	93.9 ± 0.0%	47.3 ± 0.6%	99.2 ± 0.0%	0.6 ± 0.1%
1/1	94.1 ± 0.1%	50.5 ± 1.1%	99.6 ± 0.0%	0.6 ± 0.1%
216 Colors				
1/8	22.8 ± 2.4%	5.0 ± 0.9%	45.1 ± 0.6%	43.3 ± 0.5%
1/4	79.6 ± 0.6%	60.4 ± 1.3%	89.1 ± 0.5%	81.0 ± 0.8%
1/2	86.1 ± 0.0%	74.1 ± 0.4%	94.4 ± 0.1%	88.4 ± 0.2%
1/1	88.1 ± 0.1%	77.9 ± 0.4%	96.3 ± 0.0%	90.0 ± 0.4%

Table 3. Table displaying values to form Figure 3. Accuracy for the *shape* task for different amounts of training data for the baseline model (8 colors) vs model trained on 216 colors. (a) Increasing dataset size does not increase out-of-distribution performance but rather degrades it slightly. (b) With increased *diversity* much stronger out-of-distribution generalization is achieved, with models trained on only a quarter of the data severely outperforming the 8-color baseline.

Num. Colors	Color		Shape		Size		Material	
	Test-ID	Test-OOD	Test-ID	Test-OOD	Test-ID	Test-OOD	Test-ID	Test-OOD
8	94.1 ± 0.1%	50.5 ± 1.1%	99.6 ± 0.0%	0.6 ± 0.1%	98.0 ± 0.0%	91.2 ± 1.0%	96.9 ± 0.0%	87.8 ± 0.9%
27	91.7 ± 0.0%	67.5 ± 0.7%	96.9 ± 0.1%	1.5 ± 0.1%	99.5 ± 0.0%	97.6 ± 0.0%	98.6 ± 0.0%	96.7 ± 0.1%
64	90.8 ± 0.1%	73.0 ± 0.5%	96.9 ± 0.0%	48.5 ± 0.6%	99.7 ± 0.0%	97.6 ± 0.0%	99.2 ± 0.0%	96.8 ± 0.0%
125	89.0 ± 0.1%	67.0 ± 0.3%	96.1 ± 0.1%	81.8 ± 0.6%	99.8 ± 0.0%	97.8 ± 0.0%	99.2 ± 0.0%	96.9 ± 0.0%
216	88.1 ± 0.1%	77.9 ± 0.4%	96.3 ± 0.0%	90.0 ± 0.4%	99.8 ± 0.0%	97.7 ± 0.0%	99.3 ± 0.0%	97.2 ± 0.0%

Table 4. Table displaying values to form Figure 4. Accuracy versus the number of colors in  $\mathcal{D}_{train}$  for  $\mathcal{D}_{test-ID}$  and  $\mathcal{D}_{test-OOD}$  for all tasks. Performance for the *shape* task increases drastically for the OOD split as we increase colors, increasing 86% in absolute terms over the 8-color baseline. Moreover, performance in the color task also tends to increase in the out-of-distribution split, while in-distribution only suffers slightly, even though the task becomes significantly harder. Remarkably, the *material* and *size* task rapidly increase their  $\mathcal{D}_{test-OOD}$  performance as color increases.

Num. Colors	P Bursty	Color		Shape		Size		Material	
		Test-ID	Test-OOD	Test-ID	Test-OOD	Test-ID	Test-OOD	Test-ID	Test-OOD
8	0.0	94.1 ± 0.1%	50.5 ± 1.1%	99.6 ± 0.0%	0.6 ± 0.1%	98.0 ± 0.0%	91.2 ± 1.0%	96.9 ± 0.0%	87.8 ± 0.9%
	0.5	94.2 ± 0.0%	48.9 ± 0.9%	99.6 ± 0.0%	0.9 ± 0.2%	99.5 ± 0.0%	97.6 ± 0.0%	98.6 ± 0.0%	96.7 ± 0.1%
	1.0	93.8 ± 0.0%	47.3 ± 0.1%	99.4 ± 0.0%	0.5 ± 0.0%	99.7 ± 0.0%	97.6 ± 0.0%	99.2 ± 0.0%	96.8 ± 0.0%
27	0.0	91.7 ± 0.0%	67.5 ± 0.7%	96.9 ± 0.1%	1.5 ± 0.1%	98.0 ± 0.0%	91.2 ± 1.0%	96.9 ± 0.0%	87.8 ± 0.9%
	0.5	91.7 ± 0.0%	71.9 ± 0.2%	97.1 ± 0.0%	1.8 ± 0.3%	99.5 ± 0.0%	97.6 ± 0.0%	98.6 ± 0.0%	96.7 ± 0.1%
	1.0	90.3 ± 0.0%	65.2 ± 0.8%	96.9 ± 0.0%	4.7 ± 0.4%	99.7 ± 0.0%	97.6 ± 0.0%	99.2 ± 0.0%	96.8 ± 0.0%
64	0.0	90.8 ± 0.1%	73.0 ± 0.5%	96.9 ± 0.0%	48.5 ± 0.6%	98.0 ± 0.0%	91.2 ± 1.0%	96.9 ± 0.0%	87.8 ± 0.9%
	0.5	89.8 ± 0.5%	73.8 ± 1.0%	97.0 ± 0.1%	60.5 ± 2.0%	99.5 ± 0.0%	97.6 ± 0.0%	98.6 ± 0.0%	96.7 ± 0.1%
	1.0	83.5 ± 0.2%	58.7 ± 1.0%	96.9 ± 0.1%	63.3 ± 0.9%	99.7 ± 0.0%	97.6 ± 0.0%	99.2 ± 0.0%	96.8 ± 0.0%
125	0.0	89.0 ± 0.1%	67.0 ± 0.3%	96.1 ± 0.1%	81.8 ± 0.6%	98.0 ± 0.0%	91.2 ± 1.0%	96.9 ± 0.0%	87.8 ± 0.9%
	0.5	88.9 ± 0.1%	68.5 ± 0.3%	96.8 ± 0.0%	80.6 ± 1.2%	99.5 ± 0.0%	97.6 ± 0.0%	98.6 ± 0.0%	96.7 ± 0.1%
	1.0	80.7 ± 0.2%	64.6 ± 0.3%	96.8 ± 0.0%	79.4 ± 0.5%	99.7 ± 0.0%	97.6 ± 0.0%	99.2 ± 0.0%	96.8 ± 0.0%
216	0.0	88.1 ± 0.1%	77.9 ± 0.4%	96.3 ± 0.0%	90.0 ± 0.4%	98.0 ± 0.0%	91.2 ± 1.0%	96.9 ± 0.0%	87.8 ± 0.9%
	0.5	87.3 ± 0.0%	77.7 ± 0.2%	96.7 ± 0.0%	91.4 ± 0.2%	99.5 ± 0.0%	97.6 ± 0.0%	98.6 ± 0.0%	96.7 ± 0.1%
	1.0	71.9 ± 0.2%	57.3 ± 0.4%	96.7 ± 0.0%	92.4 ± 0.3%	99.7 ± 0.0%	97.6 ± 0.0%	99.2 ± 0.0%	96.8 ± 0.0%

Table 5. Table displaying values to form Figure 5. Accuracy for all tasks in test-ID and test-OOD for different levels of *burstiness* over *color* for various numbers of colors. Limiting the number of colors available for each image during training allows the model to gain up to 14.8% more accuracy over the baseline. The *color* task, however, suffers up to 14.3% decline as the *color* task becomes easier to memorize.

Num. Colors	Jitter	Color		Shape		Size		Material	
		Test-ID	Test-OOD	Test-ID	Test-OOD	Test-ID	Test-OOD	Test-ID	Test-OOD
8	0.00	94.1 ± 0.1%	50.5 ± 1.1%	99.6 ± 0.0%	0.6 ± 0.1%	98.0 ± 0.0%	91.2 ± 1.0%	96.9 ± 0.0%	87.8 ± 0.9%
	0.05	94.1 ± 0.1%	46.6 ± 0.4%	99.6 ± 0.0%	0.4 ± 0.0%	99.5 ± 0.0%	97.6 ± 0.0%	98.6 ± 0.0%	96.7 ± 0.1%
	0.10	94.1 ± 0.1%	48.0 ± 0.7%	99.6 ± 0.0%	0.9 ± 0.2%	99.7 ± 0.0%	97.6 ± 0.0%	99.2 ± 0.0%	96.8 ± 0.0%
	0.50	93.9 ± 0.0%	47.1 ± 0.4%	99.7 ± 0.0%	0.3 ± 0.1%	99.8 ± 0.0%	97.8 ± 0.0%	99.2 ± 0.0%	96.9 ± 0.0%
27	0.00	91.7 ± 0.0%	67.5 ± 0.7%	96.9 ± 0.1%	1.5 ± 0.1%	98.0 ± 0.0%	91.2 ± 1.0%	96.9 ± 0.0%	87.8 ± 0.9%
	0.05	91.9 ± 0.0%	69.4 ± 1.5%	97.4 ± 0.0%	1.4 ± 0.2%	99.5 ± 0.0%	97.6 ± 0.0%	98.6 ± 0.0%	96.7 ± 0.1%
	0.10	91.8 ± 0.1%	68.4 ± 1.0%	97.3 ± 0.1%	1.7 ± 0.2%	99.7 ± 0.0%	97.6 ± 0.0%	99.2 ± 0.0%	96.8 ± 0.0%
	0.50	91.9 ± 0.0%	66.1 ± 2.0%	97.2 ± 0.0%	1.1 ± 0.2%	99.8 ± 0.0%	97.8 ± 0.0%	99.2 ± 0.0%	96.9 ± 0.0%
64	0.00	90.8 ± 0.1%	73.0 ± 0.5%	96.9 ± 0.0%	48.5 ± 0.6%	98.0 ± 0.0%	91.2 ± 1.0%	96.9 ± 0.0%	87.8 ± 0.9%
	0.05	90.9 ± 0.0%	68.5 ± 0.6%	97.1 ± 0.0%	57.1 ± 0.1%	99.5 ± 0.0%	97.6 ± 0.0%	98.6 ± 0.0%	96.7 ± 0.1%
	0.10	91.0 ± 0.0%	67.1 ± 0.3%	97.3 ± 0.0%	62.3 ± 3.0%	99.7 ± 0.0%	97.6 ± 0.0%	99.2 ± 0.0%	96.8 ± 0.0%
	0.50	91.1 ± 0.0%	68.6 ± 0.6%	97.8 ± 0.0%	63.8 ± 0.9%	99.8 ± 0.0%	97.8 ± 0.0%	99.2 ± 0.0%	96.9 ± 0.0%
125	0.00	89.0 ± 0.1%	67.0 ± 0.3%	96.1 ± 0.1%	81.8 ± 0.6%	98.0 ± 0.0%	91.2 ± 1.0%	96.9 ± 0.0%	87.8 ± 0.9%
	0.05	89.8 ± 0.0%	71.1 ± 0.4%	96.8 ± 0.1%	85.0 ± 0.5%	99.5 ± 0.0%	97.6 ± 0.0%	98.6 ± 0.0%	96.7 ± 0.1%
	0.10	89.7 ± 0.1%	68.4 ± 0.5%	96.7 ± 0.1%	79.2 ± 0.7%	99.7 ± 0.0%	97.6 ± 0.0%	99.2 ± 0.0%	96.8 ± 0.0%
	0.50	89.8 ± 0.1%	70.6 ± 1.1%	96.9 ± 0.0%	85.8 ± 0.9%	99.8 ± 0.0%	97.8 ± 0.0%	99.2 ± 0.0%	96.9 ± 0.0%
216	0.00	88.1 ± 0.1%	77.9 ± 0.4%	96.3 ± 0.0%	90.0 ± 0.4%	98.0 ± 0.0%	91.2 ± 1.0%	96.9 ± 0.0%	87.8 ± 0.9%
	0.05	88.4 ± 0.0%	79.8 ± 0.3%	96.8 ± 0.1%	92.2 ± 0.1%	99.5 ± 0.0%	97.6 ± 0.0%	98.6 ± 0.0%	96.7 ± 0.1%
	0.10	88.0 ± 0.1%	75.6 ± 0.2%	96.4 ± 0.1%	91.0 ± 0.3%	99.7 ± 0.0%	97.6 ± 0.0%	99.2 ± 0.0%	96.8 ± 0.0%
	0.50	88.4 ± 0.1%	78.7 ± 0.7%	96.7 ± 0.1%	92.0 ± 0.1%	99.8 ± 0.0%	97.8 ± 0.0%	99.2 ± 0.0%	96.9 ± 0.0%

Table 6. Table displaying values to form Figure 6. Accuracy after applying latent intervention for all tasks in test-ID and test-OOD for different levels of latent intervention of the *color* latent attribute for various numbers of colors. Altering the color hue randomly during training allows the model to gain up to 15% more out-of-distribution accuracy over the baseline.

Num. Colors	Hidden Size	Color		Shape		Size		Material	
		Test-ID	Test-OOD	Test-ID	Test-OOD	Test-ID	Test-OOD	Test-ID	Test-OOD
8	32	79.3 ± 0.1%	4.6 ± 0.6%	90.8 ± 0.8%	0.0 ± 0.0%	98.0 ± 0.0%	91.2 ± 1.0%	96.9 ± 0.0%	87.8 ± 0.9%
	64	87.0 ± 1.6%	18.1 ± 1.9%	98.1 ± 0.4%	0.0 ± 0.0%	99.5 ± 0.0%	97.6 ± 0.0%	98.6 ± 0.0%	96.7 ± 0.1%
	128	93.8 ± 0.1%	43.9 ± 0.7%	99.5 ± 0.0%	0.2 ± 0.0%	99.7 ± 0.0%	97.6 ± 0.0%	99.2 ± 0.0%	96.8 ± 0.0%
	256	94.1 ± 0.1%	50.5 ± 1.1%	99.6 ± 0.0%	0.6 ± 0.1%	99.8 ± 0.0%	97.8 ± 0.0%	99.2 ± 0.0%	96.9 ± 0.0%
216	256	88.1 ± 0.1%	77.9 ± 0.4%	96.3 ± 0.0%	90.0 ± 0.4%	98.0 ± 0.0%	91.2 ± 1.0%	96.9 ± 0.0%	87.8 ± 0.9%
	512	88.8 ± 0.0%	81.6 ± 0.2%	97.3 ± 0.0%	93.5 ± 0.1%	99.5 ± 0.0%	97.6 ± 0.0%	98.6 ± 0.0%	96.7 ± 0.1%
	1024	89.1 ± 0.1%	82.2 ± 0.1%	97.6 ± 0.0%	92.4 ± 0.2%	99.7 ± 0.0%	97.6 ± 0.0%	99.2 ± 0.0%	96.8 ± 0.0%

Table 7. Table displaying values to form Figure 7. In-Distribution and Out-of-Distribution accuracy for models trained with different values for their hidden dimensions on a training set with 8 and 216 colors for all tasks.